A&A 459, 21–30 (2006)
DOI: 10.1051/0004-6361:20066055
© ESO 2006

Astronomy & Astrophysics

Unveiling the nature of *INTEGRAL* objects through optical spectroscopy

V. Identification and properties of 21 southern hard X-ray sources⋆,⋆⋆

N. Masetti[1], L. Morelli[2], E. Palazzi[1], G. Galaz[2], L. Bassani[1], A. Bazzano[3], A. J. Bird[4], A. J. Dean[4], G. L. Israel[5], R. Landi[1], A. Malizia[1], D. Minniti[2], F. Schiavone[1], J. B. Stephen[1], P. Ubertini[3], and R. Walter[6]

[1] INAF – Istituto di Astrofisica Spaziale e Fisica Cosmica di Bologna, Via Gobetti 101, 40129 Bologna, Italy
(formerly IASF/CNR, Bologna)
e-mail: masetti@iasfbo.inaf.it
[2] Departamento de Astronomía y Astrofísica, Pontificia Universidad Católica de Chile, Casilla 306, Santiago 22, Chile
[3] INAF – Istituto di Astrofisica Spaziale e Fisica Cosmica di Roma, Via Fosso del Cavaliere 100, 00133 Rome, Italy
(formerly IASF/CNR, Rome)
[4] School of Physics & Astronomy, University of Southampton, Southampton, Hampshire, SO17 1BJ, UK
[5] INAF – Osservatorio Astronomico di Roma, via Frascati 33, 00040 Monteporzio Catone, Italy
[6] INTEGRAL Science Data Centre, Chemin d'Ecogia 16, 1290 Versoix, Switzerland

Received 17 July 2006 / Accepted 2 August 2006

ABSTRACT

Optical spectroscopic identification of the nature of 21 unidentified southern hard X-ray objects is reported here in the framework of our campaign aimed at determining the nature of newly-discovered and/or unidentified sources detected by *INTEGRAL*. Our results show that 5 of these objects are magnetic Cataclysmic Variables (CVs), 4 are High-Mass X-ray Binaries (HMXBs; one of which is in the Large Magellanic Cloud) and 12 are Active Galactic Nuclei (AGNs). When feasible, the main physical parameters for these hard X-ray sources are also computed using the multiwavelength information available in the literature. These identifications further underscore the importance of *INTEGRAL* in the study of the hard X-ray spectrum of AGNs, HMXBs and CVs, and the usefulness of a strategy of catalogues cross-correlation plus optical spectroscopy to securely pinpoint the actual nature of the X-ray sources detected with *INTEGRAL*.

Key words. galaxies: Seyfert – stars: novae, cataclysmic variables – X-rays: binaries – techniques: spectroscopic – X-rays: general

1. Introduction

Since its launch in October 2002, the *INTEGRAL* satellite (Winkler et al. 2003) is boosting our knowledge of the hard X-ray sky above 20 keV in terms of both sensitivity and positional accuracy of the detected sources. Thanks to the capabilities of the IBIS instrument (Ubertini et al. 2003), *INTEGRAL* is effectively detecting hard X-ray objects at the mCrab level with a typical localization accuracy of 2−3′ (Gros et al. 2003). This has made it possible, for the first time, to obtain all-sky maps in the 20−100 keV range with arcminute accuracy and down to mCrab sensitivities (e.g., Bird et al. 2006).

Most of the sources detected by *INTEGRAL* are known Galactic X-ray binaries (∼50% of the total number of detected objects), plus a fraction of known Active Galactic Nuclei (AGNs; ∼10%) and Cataclysmic Variables (CVs; ∼5%). However, a large majority of the remaining objects (about 25% of all detections achieved with IBIS) has no obvious counterpart at other wavelengths and therefore cannot immediately be associated with any known class of high-energy emitting objects.

Recently, in order to fill this identification gap, we started a campaign aimed at identifying the nature of these still unknown sources through optical spectroscopy at northern and southern telescopes (Masetti et al. 2004, 2006a,b,c; hereafter Papers I–IV). Our results indicate that, despite *INTEGRAL* doubled the number of Galactic High Mass X-ray Binaries (HMXBs; see Walter et al. 2006) and despite the expectation according to which most of these unidentified objects should be HMXBs (Dean et al. 2005), about half of them are actually identified in the optical as nearby ($z \lesssim 0.1$) AGNs (Papers I–IV).

In the framework of our continuing effort to identify unknown *INTEGRAL* sources, we present here the optical spectroscopic observations obtained on 21 southern objects at the 1.5-metre telescope of the Cerro Tololo Interamerican Observatory (CTIO) located in Cerro Tololo (Chile). In Sect. 2 we introduce the criteria with which the sample of *INTEGRAL* and optical objects was chosen for the present observational campaign, whereas in Sect. 3 a description of the observations is given; Sect. 4 reports and discusses the results, divided into three broad classes of sources (CVs, HMXBs and AGNs), together with a statistical outline of the identifications of *INTEGRAL* sources obtained up to now. Conclusions are drawn in Sect. 5.

⋆ Based on observations collected at the Cerro Tololo Interamerican Observatory (Chile).

⋆⋆ Table 1, Figs. 1 and 2 are only available in electronic form at http://www.aanda.org

Article published by EDP Sciences and available at http://www.aanda.org or http://dx.doi.org/10.1051/0004-6361:20066055

2. Sample selection

In order to continue our program (Papers I–IV) of optical spectroscopic identifications of *INTEGRAL* sources with unknown nature, we first collected all objects belonging to the 2nd IBIS Galactic Plane Survey (Bird et al. 2006), to the Crux arm Tangent Survey (Revnivtsev et al. 2006a), to the AGN minisurvey of Sazonov et al. (2005) and to the Circinus-Carina arm Survey (Kuiper et al. 2006), and which are visible from the southern hemisphere.

We then positionally cross-correlated the IBIS error circles of the selected southern unidentified *INTEGRAL* objects with catalogues of soft (<10 keV) X-ray sources. This was made in order to reduce the X-ray error box size to some ($\lesssim$10) arcsec at most. For the present sample, we selected *INTEGRAL* objects with a single *ROSAT* source (Voges et al. 1999, 2000; *ROSAT* Team 2000), or a single *Swift*/XRT archival X-ray source (available at `http://www.asdc.asi.it`), or a single *Chandra* source (Sazonov et al. 2005; Halpern 2005; Tomsick et al. 2006; Israel et al., in preparation) within the IBIS error box. This approach was chosen because Stephen et al. (2005, 2006) show that, from a statistical argument, these are very likely to be the soft X-ray counterparts of the positionally corresponding *INTEGRAL* sources; besides, the results of Papers I–IV prove that this approach is very effective, when combined with optical spectroscopy.

For the cross-correlation searches, we considered 90% confidence level *INTEGRAL*/IBIS error circles. To this aim, a conservative 90% confidence level error box radius of 2′ was assumed for the objects belonging to the 2nd IBIS Galactic Plane Survey (Bird et al. 2006), and of 6′ for the Crux arm Survey objects (as stated in Revnivtsev et al. 2006a). For the Circinus-Carina Survey sources, the 90% confidence level error box radius as reported in Kuiper et al. (2006) regarding each object was considered.

In this way we could select 18 unidentified *INTEGRAL* sources associated with a single arcsec-sized soft X-ray error box which, when overlaid onto the corresponding DSS-II-Red survey[1] images, is seen to contain a single or few (3 at most) relatively bright ($R < 18$) possible optical counterparts. Three additional sources (IGR J14175−4641, IGR J14552−5133 and IGR J18244−5622) were added to our sample as their IBIS error circle includes bright field objects which were suggested as their possible counterparts (Revnivtsev et al. 2006a,b). We refer the reader to Paper III for the caveats of choosing, within the IBIS error box, "peculiar" sources which are not readily associated with an arcsec-sized soft X-ray position.

The list of selected *INTEGRAL* sources is shown in the leftmost column of Table 1. Figures 1 and 2 report the optical DSS-II-Red survey fields of the 14 sources (out of the 21 of the selected sample) for which no optical finding chart was published before the present work. In these figures, the position of the proposed counterpart of each *INTEGRAL* source is also shown (see also Table 2). The finding charts of the remaining sources can be found in Sazonov et al. (2005), Tomsick et al. (2006) and Revnivtsev et al. (2006b).

In the following, when not explicitly stated otherwise, for our X-ray flux estimates we will assume a Crab-like spectrum. We also remark that the results presented here supersede the preliminary ones of Masetti et al. (2006d).

[1] Available at `http://archive.eso.org/dss/dss`

Table 2. Equatorial J2000 coordinates of the counterparts to the *INTEGRAL* sources of the sample presented in this paper and lacking an accurate (arcsecond or better) position up to now. Coordinates (from the 2MASS catalogue) have an accuracy better than 0.″1, with the exception of those for IGR J14552−5133, which were extracted from the DSS-II-Red astrometry and have ∼1″ accuracy.

Object	RA (J2000)	Dec (J2000)
IGR J07597−3842	$07^h59^m41\overset{s}{.}819$	$-38°43'56\overset{''}{.}03$
IGR J10101−5654	$10^h10^m11\overset{s}{.}866$	$-56°55'32\overset{''}{.}06$
XSS J12270−4859	$12^h27^m58\overset{s}{.}748$	$-48°53'42\overset{''}{.}88$
IGR J14175−4641	$14^h17^m03\overset{s}{.}662$	$-46°41'41\overset{''}{.}19$
IGR J14471−6319	$14^h47^m14\overset{s}{.}881$	$-63°17'19\overset{''}{.}24$
IGR J14515−5542	$14^h51^m33\overset{s}{.}131$	$-55°40'38\overset{''}{.}40$
IGR J14536−5522	$14^h53^m41\overset{s}{.}055$	$-55°21'38\overset{''}{.}74$
IGR J14552−5133	$14^h55^m17\overset{s}{.}8$	$-51°34'17''$
IGR J15094−6649	$15^h09^m26\overset{s}{.}013$	$-66°49'23\overset{''}{.}29$
IGR J16185−5928	$16^h18^m36\overset{s}{.}441$	$-59°27'17\overset{''}{.}36$
IGR J16558−5203	$16^h56^m05\overset{s}{.}618$	$-52°03'40\overset{''}{.}87$
IGR J17200−3116	$17^h20^m05\overset{s}{.}913$	$-31°16'59\overset{''}{.}65$
IGR J17488−3253	$17^h48^m55\overset{s}{.}129$	$-32°54'52\overset{''}{.}15$
IGR J17513−2011	$17^h51^m13\overset{s}{.}623$	$-20°12'14\overset{''}{.}58$

3. Optical spectroscopy

All objects were observed spectroscopically with the 1.5-metre CTIO telescope of Cerro Tololo (Chile) equipped with the R-C spectrograph, which carries a 1274 × 280 pixels Loral CCD. Data were acquired using Grating #13/I and with a slit width of 1.″5, giving a nominal spectral coverage between 3300 and 10 500 Å and a dispersion of 5.7 Å/pix. The complete log of the observations is reported in Table 1.

After cosmic-ray rejection, the spectra were reduced, background subtracted and optimally extracted (Horne 1986) using IRAF[2]. Wavelength calibration was performed using He-Ar lamps acquired soon after each spectroscopic exposure; the spectra were then flux-calibrated using the spectrophotometric standards LTT 3218 and LTT 7379 (Hamuy et al. 1992, 1994).

Finally, and when applicable, different spectra of the same object were stacked together to increase the S/N ratio. The wavelength calibration uncertainty was ∼0.5 Å for all cases; this was checked using the positions of background night sky lines.

4. Results

In this section we present the results of our spectroscopic campaign at CTIO. The optical magnitudes quoted below, if not otherwise stated, are extracted from the USNO-A2.0[3] catalogue.

For the determination of the distance of compact Galactic X-ray sources, in the case of CVs we will assume an absolute magnitude $M_V \sim 9$ and an intrinsic color index $(V-R)_0 \sim 0$ mag (Warner 1995), whereas for HMXBs, when applicable, we will use the intrinsic stellar color indices and absolute magnitudes as reported in Lang (1992) and Wegner (1994).

When applicable, for the calculation of the absorption local to an AGN host galaxy, we first dereddened the H_α and H_β line

[2] IRAF is the Image Reduction and Analysis Facility made available to the astronomical community by the National Optical Astronomy Observatories, which are operated by AURA, Inc., under contract with the U.S. National Science Foundation. It is available at `http://iraf.noao.edu/`

[3] Available at `http://archive.eso.org/skycat/servers/usnoa/`

fluxes by applying a correction for the Galactic absorption along the source line of sight. This was done following the prescription for the computation of the Galactic color excess $E(B-V)_{\rm Gal}$ as in Schlegel et al. (1998), and considering the Galactic extinction law of Cardelli et al. (1989). Then, we assumed an intrinsic H_α/H_β line ratio of 2.86 (Osterbrock 1989) and we computed the color excess $E(B-V)_{\rm AGN}$ local to the AGN host, using again the Cardelli et al.'s (1989) extinction law, from the comparison between the intrinsic line ratio and the one corrected for the Galactic reddening.

The spectra of the galaxies shown here were not corrected for starlight contamination (see, e.g., Ho et al. 1993, 1997) given their limited S/N and resolution. We do not consider this to affect any of our conclusions. In the following we assume a cosmology with $H_0 = 65$ km s^{-1} Mpc^{-1}, $\Omega_\Lambda = 0.7$ and $\Omega_{\rm m} = 0.3$.

For the AGN classification, we used the criteria of Veilleux & Osterbrock (1987) and the line ratio diagnostics of Ho et al. (1993, 1997); moreover, for the subclass assignation of Seyfert 1 nuclei, we used the H_β/[O III]λ5007 line flux ratio criterion as per Winkler (1992).

In Table 2 we report the equatorial J2000 coordinates of the proposed optical counterparts lacking up to now a precise (i.e. at one-arcsecond accuracy or better) position; we also show these objects in Figs. 1 and 2. This information is extracted from the 2MASS catalogue (with $\lesssim$0.″1 accuracy, according to Skrutskie et al. 2006) but for IGR J14552−5133, for which the DSS-II-Red astrometry (which has ∼1″ accuracy) was used as no entry is present for this source in the 2MASS catalogue. The accurate coordinates of the 7 objects not included in Table 2 are reported in Tomsick et al. (2006), Sazonov et al. (2005) and Revnivtsev et al. (2006b).

In the following Subsections we give the object identifications divided into three broad classes (CVs, HMXBs and AGNs) ordered according to their increasing distance from Earth.

4.1. CVs

Five objects of our sample (XSS J12270−4859, IGR J14536−5522, IGR J15094−6649, IGR J16167−4957 and IGR J17195−4100) were identified as CVs through the appearance of their optical spectra (Fig. 3). All of them show Balmer emissions up to at least H_δ, as well as several He I and He II lines in emission. All of the detected lines are consistent with being at $z = 0$, indicating that these objects belong to our Galaxy.

The *ROSAT* error circle of IGR J15094−6649 (see Fig. 2, upper middle panel) actually contains two relatively bright ($R <$ 18) objects: simultaneous optical spectroscopy shows that the true counterpart is the brighter one (the coordinates of which are reported in Table 2), while the other is a normal Galactic star with no peculiarities, thus unrelated with the *INTEGRAL* hard X-ray source.

The main spectral characteristics for each object, and the parameters which can be inferred from the optical and X-ray observational data, are listed in Table 3. The facts that, in the spectra of all these 5 objects, the Balmer decrement clearly appears negative, the He IIλ4686/H_β Equivalent Width (*EW*) ratio is $\gtrsim$0.5 and the *EW*s of He II and H_β are around (or larger than) 10 Å indicate that these sources are magnetic CVs belonging to the Intermediate Polar (IP) subclass (see Warner 1995, and references therein). Their optical spectra, moreover, closely resemble that of another CV detected with *INTEGRAL*, IGR J00234+6141 (den Hartog et al. 2006; Halpern & Mirabal 2006; Paper IV), which was classified as an IP as well (Paper IV; Bikmaev et al. 2006).

The large (>20 Å) *EW*s observed in the He II λ4686 and H_β lines of the spectrum of the optical counterpart of IGR J14536−5522 may indicate an even stronger magnetic field of the accreting white dwarf harboured in this system. This fact may suggest that this object is perhaps a Polar, rather than an IP, CV (Warner 1995).

Given that, with the exception of IGR J16167−4957, the observed H_α/H_β flux ratio is always <1.5, we assumed $A_{\rm V} = 0$ mag for the computation of the distance to each CV (see Table 3). For IGR J16167−4957 we instead considered $A_{\rm V} = 1.3$ mag, inferred by Tomsick et al. (2006) from a multiwavelength study of this source. The X-ray luminosities for the various objects were then computed using the fluxes reported in Bird et al. (2006), Kuiper et al. (2006) and Tomsick et al. (2006).

4.2. HMXBs

We identify 4 of the *INTEGRAL* sources of our sample as HMXBs by their overall spectral appearance (see Fig. 4), which is typical of this class of objects (see e.g. Paper III), with narrow H_α emission at a wavelength consistent with that of the laboratory restframe, superimposed on an intrinsically blue continuum with Balmer absorptions. In three cases out of four (IGR J10101−5654, IGR J16207−5129 and IGR J17200−3116), however, the stellar continuum appears strongly reddened and almost undetected blueward of 5000 Å, implying the presence of substantial interstellar dust along the line of sight. This also is quite typical of HMXBs detected with *INTEGRAL* (e.g., 2RXP J130159.6−635806; Paper III) and indicates that these objects are relatively far from Earth.

In the case of IGR J05007−7047 we detect the H_α line in emission, and the rest of the Balmer series (up to H_ζ) in absorption, all redshifted of ∼6 Å with respect to the corresponding laboratory wavelengths. This is consistent with the redshift of the Large Magellanic Cloud (LMC; see Cusumano et al. 1998, and references therein); thus, we confirm the hypothesis put forward by Sazonov et al. (2005) and Götz et al. (2006) that this hard X-ray source is indeed a HMXB belonging to the LMC.

We here note that the *Swift* error circle of IGR J10101−5654 (Fig. 1, upper middle panel) marginally encompasess a relatively bright object: in this case also our optical spectroscopy, acquired simultaneously with that of the true counterpart, shows that it is a normal mid-type Galactic star.

Table 4 collects the relevant optical spectral information on these 4 sources, along with their main parameters inferred from the available optical and X-ray data. Luminosities for each object were calculated using the X-ray fluxes in Bird et al. (2006) and Tomsick et al. (2006).

Concerning IGR J05007−7047, optical photometry was obtained from Massey (2002), and a distance of 50 kpc was assumed.

For IGR J16207−5129, thanks to the subarcsec *Chandra* position of Tomsick et al. (2006), we revise the identification given in Paper III: this object is still a HMXB, but is not connected at all with star HD 146803 (which lies in the IBIS error box, but it is not consistent with the *Chandra* soft X-ray position). Assuming $A_{\rm V} = 10.8$ (Tomsick et al. 2006), we determine for this source the parameter values reported in Table 4.

Unfortunately, due to the lack of reliable optical photometry for the optical counterparts of IGR J10101−5654 and IGR J17200−3116, no significant information concerning

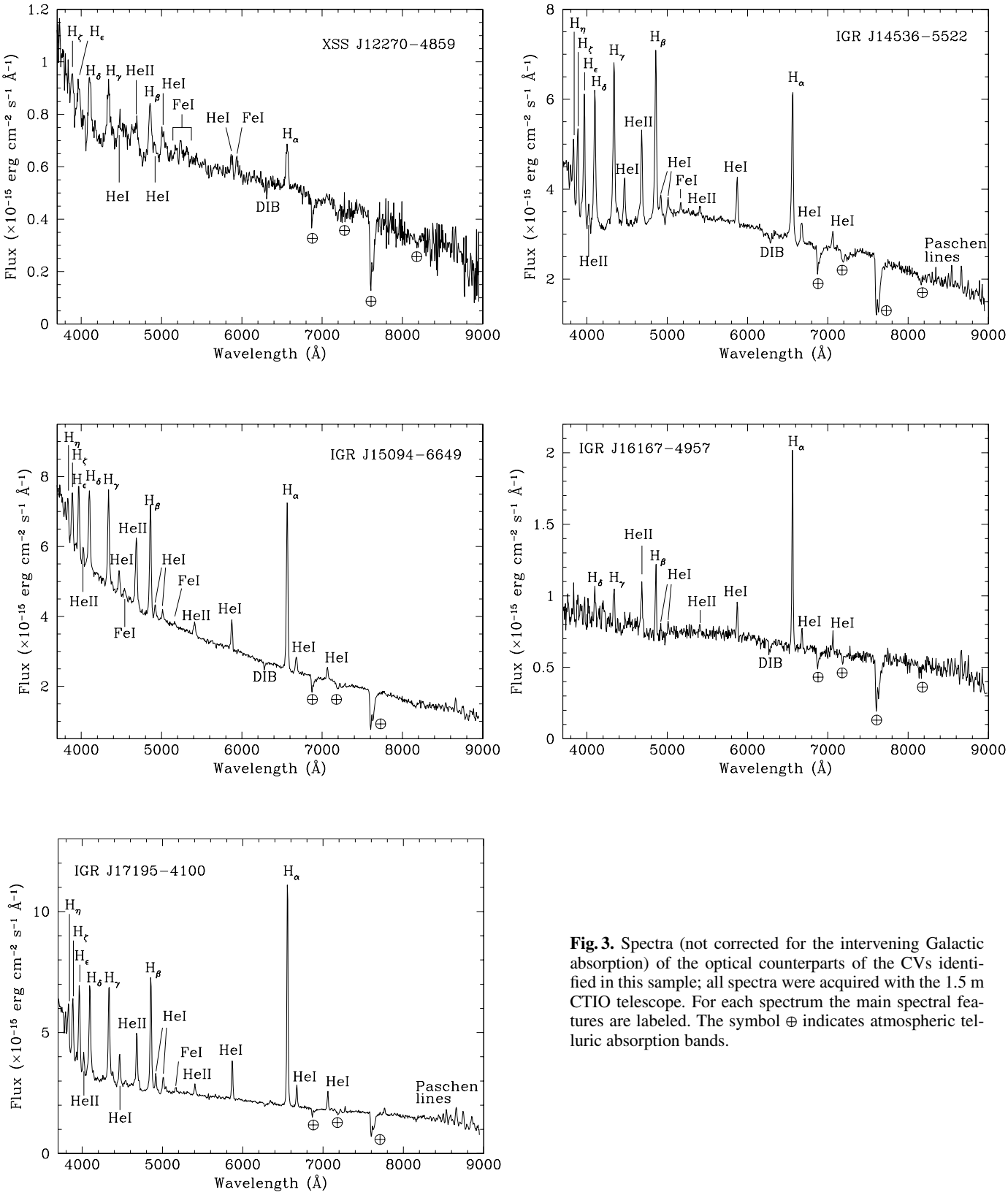

Fig. 3. Spectra (not corrected for the intervening Galactic absorption) of the optical counterparts of the CVs identified in this sample; all spectra were acquired with the 1.5 m CTIO telescope. For each spectrum the main spectral features are labeled. The symbol ⊕ indicates atmospheric telluric absorption bands.

distance, spectral type and X-ray luminosity can be determined for these two objects. Nevertheless, the H_α *EW* we measure for IGR J10101−5654 appears too large for a supergiant secondary star (see Leitherer 1988). Thus, we infer that this HMXB hosts a secondary of intermediate luminosity class.

Table 3. Synoptic table containing the main results concerning the 5 CVs discovered in the present sample of *INTEGRAL* sources. *EW*s are expressed in Å, line fluxes are in units of 10^{-14} erg cm^{-2} s^{-1}, whereas X-ray luminosities are in units of 10^{32} erg s^{-1} and the reference band (between brackets) is expressed in keV.

Object	H_α		H_β		He II λ4686		R	d	L_X
	EW	Flux	*EW*	Flux	*EW*	Flux	mag	(pc)	
XSS J12270−4859	10.2 ± 0.8	0.54 ± 0.04	11.6 ± 1.7	0.75 ± 0.11	12.4 ± 1.9	0.83 ± 0.12	15.7	∼220	0.11 (0.1–2.4) 1.4 (17–60)
IGR J14536−5522	29 ± 1	8.6 ± 0.3	30.4 ± 1.5	10.0 ± 0.5	20.3 ± 1.4	5.2 ± 0.4	15.4	∼190	0.15 (0.1–2.4) 1.3 (20–65)
IGR J15094−6649	45 ± 2	11.1 ± 0.6	19.6 ± 1.0	7.9 ± 0.4	12.8 ± 0.6	5.5 ± 0.3	14.7	∼140	0.027 (0.1–2.4) 0.35 (17–60)
IGR J16167−4957	39 ± 3	2.46 ± 0.17	11.2 ± 1.1	0.84 ± 0.08	10.5 ± 1.1	0.79 ± 0.08	16.2	∼170	1.5 (0.5–10) 0.55 (20–40) <0.33 (40–100)
IGR J17195−4100	85 ± 3	16.7 ± 0.5	41 ± 2	10.6 ± 0.5	18.5 ± 0.9	5.5 ± 0.3	14.3	∼110	0.36 (0.5–10) 0.55 (20–100)

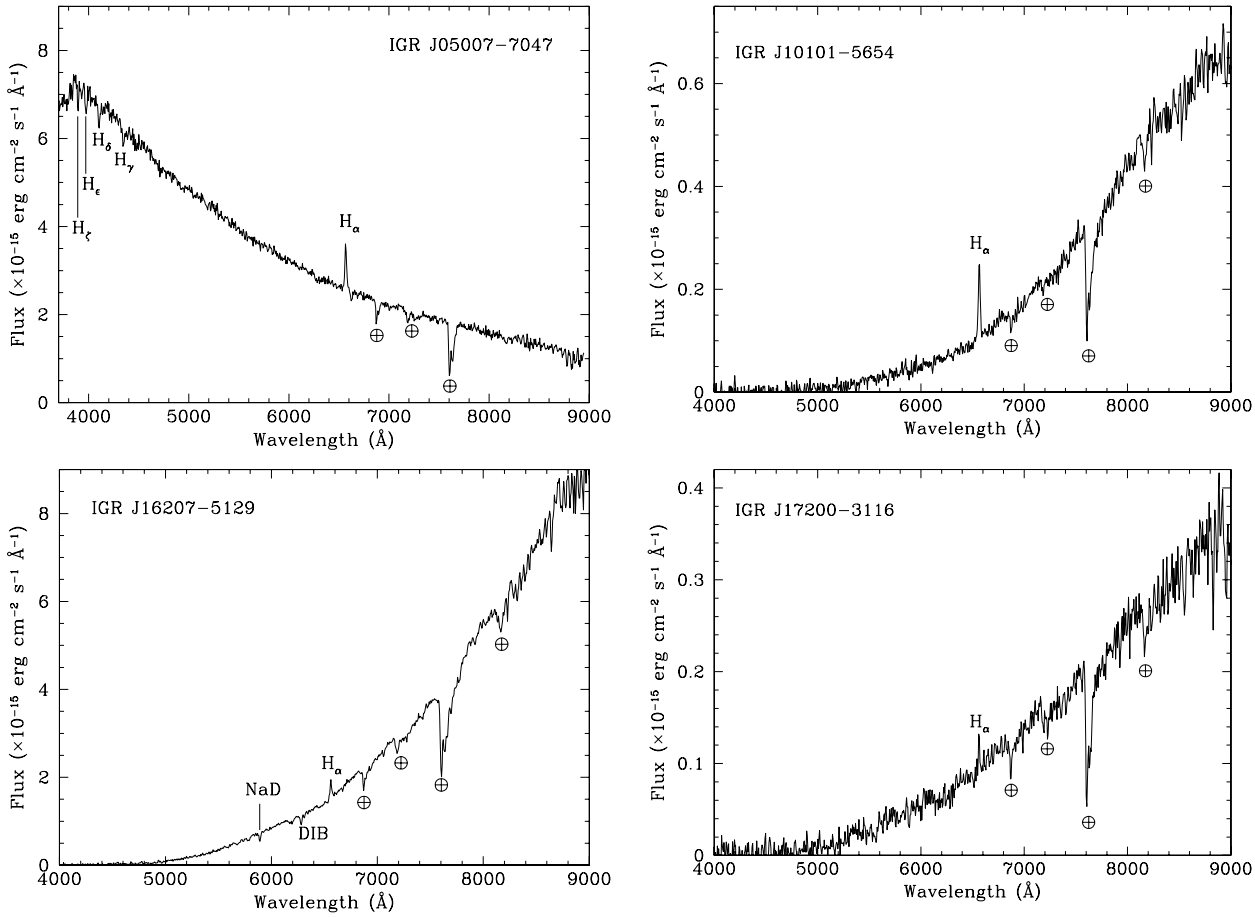

Fig. 4. Spectra (not corrected for the intervening Galactic absorption) of the optical counterparts of the HMXBs identified in this sample; all spectra were acquired with the 1.5 m CTIO telescope. For each spectrum the main spectral features are labeled. The symbol ⊕ indicates atmospheric telluric absorption bands.

4.3. AGNs

The remaining 12 objects of our sample show optical spectra which are dominated by redshifted broad and/or narrow emission lines typical of AGNs. We classify half of this subsample (6 objects) as Seyfert 2 galaxies; the other half is made of Seyfert 1 galaxies. Of these latter ones, 2 are classified as Seyfert 1.2, one as Seyfert 1.9 and two as Narrow-Line (NL) Seyfert 1; for the case of IGR J17488−3253 only a general Seyfert 1 classification can be given due to the lower quality of the spectrum (see Fig. 6, central right panel). The main observed and inferred parameters for each object are reported in Table 5. We assumed a null local absorption for Seyfert 1 AGNs. In the table, X-ray luminosities were computed using the fluxes reported in Bird et al. (2006), Kuiper et al. (2006), Sazonov et al. (2005) and Revnivtsev et al. (2006a,b), and using the *ROSAT* countrates (Voges et al. 1999, 2000; *ROSAT* Team 2000).

One can note that the *ROSAT* error circles of IGR J14471−6319 (Fig. 1, central middle panel) and

Table 4. Synoptic table containing the main results concerning the 4 HMXBs discovered in the present sample of *INTEGRAL* sources. *EW*s are expressed in Å, line fluxes are in units of 10^{-14} erg cm^{-2} s^{-1}, whereas X-ray luminosities are in units of 10^{36} erg s^{-1} and the reference band (between brackets) is expressed in keV.

Object	H_α		Optical	A_V	d	Spectral	L_X
	EW	Flux	mag.	(mag)	(kpc)	type	
IGR J05007−7047	8.8 ± 0.4	2.3 ± 0.1	14.8 (*V*)	0.38	50	B2 III	0.91[a] (0.5–8) 3.6[a] (17–60)
IGR J10101−5654	34 ± 4	0.33 ± 0.04	–	–	–	early giant	–
IGR J16207−5129	5.0 ± 0.3	0.76 ± 0.04	∼15.6 (*R*)	10.8	∼4.6[b]	early supergiant	0.11 (0.3–10) 0.12 (20–100)
IGR J17200−3116	5.5 ± 1.1	0.05 ± 0.01	–	–	–	–	–

[a] Luminosity estimate from Sazonov et al. (2005). [b] Assuming $(V - R)_0 \sim -0.1$

Table 5. Synoptic table containing the main results concerning the 12 AGNs discovered in the present sample of *INTEGRAL* sources. Emission line fluxes are reported both as observed and (between square brackets) corrected for the intervening Galactic absorption $E(B - V)_{Gal}$ along the object line of sight. Line fluxes are in units of 10^{-14} erg cm^{-2} s^{-1}, whereas X-ray luminosities are in units of 10^{43} erg s^{-1} and the reference band (between round brackets) is expressed in keV. Errors and limits are at 1σ and 3σ confidence levels, respectively. The typical error on the redshift measurement is ±0.001.

Object	F_{H_α}	F_{H_β}	$F_{[OIII]}$	Class	z	D_L	$E(B-V)$		L_X
						(Mpc)	Gal.	AGN	
IGR J07565−4139	0.56 ± 0.08 [7.0 ± 1.0]	<0.05 [<0.6]	<0.04 [<0.4]	Sy2	0.021	98.4	0.77	>1.4	0.41 (0.5–8) 1.7 (17–60) 0.88 (20–40) <0.87 (40–100)
IGR J07597−3842	* *	4.9 ± 0.5 [61 ± 6]	2.1 ± 0.2 [25 ± 3]	Sy1.2	0.040	190.1	0.81	0	3.5 (0.1–2) 15.3 (20–100)
IGR J12026−5349	4.6 ± 0.4 [7.6 ± 0.7]	0.5 ± 0.1 [1.0 ± 0.2]	9.1 ± 0.5 [17.5 ± 0.9]	Sy2	0.028	131.4	0.21	1.0	1.4 (0.5–8) 6.8 (17–60)
IGR J14175−4641	0.64 ± 0.13 [0.79 ± 0.16]	in abs. ″	0.18 ± 0.04 [0.24 ± 0.05]	Sy2	0.076	370.6	0.11	–	27.1 (17–60)
IGR J14471−6319	0.17 ± 0.02 [7.6 ± 1.1]	<0.02 [<1.5]	<0.02 [<1.1]	Sy2	0.038	180.4	1.31	>0.58	0.044 (0.1–2.4) 4.8 (17–60)
IGR J14515−5542	0.45 ± 0.09 [2.9 ± 0.6]	<0.03 [<3.0]	0.18 ± 0.04 [6.4 ± 1.6]	Sy2	0.018	84.2	1.13	–	0.11 (0.1–2.4) 1.8 (20–65)
IGR J14552−5133	* *	1.81 ± 0.12 [14.8 ± 1.0]	1.26 ± 0.07 [10.2 ± 0.7]	NL Sy1	0.016	74.7	0.67	0	0.079 (0.1–2.4) 0.92 (17–60)
IGR J16185−5928	* *	6.0 ± 0.3 [16.0 ± 0.8]	1.21 ± 0.15 [3.2 ± 0.4]	NL Sy1	0.035	165.8	0.32	0	0.50 (0.1–2.4) 5.4 (17–60)
IGR J16558−5203	* *	14.6 ± 0.8 [53 ± 3]	3.9 ± 0.3 [14.7 ± 1.0]	Sy1.2	0.054	259.3	0.44	0	3.0 (0.1–2.4) 27.4 (20–100)
IGR J17488−3253	* *	<0.08 [<10]	<0.1 [<16]	Sy1	0.020	93.7	1.63	0	0.098 (0.1–2.4) 5.1 (20–100)
IGR J17513−2011	* *	0.047 ± 0.014 [2.3 ± 0.7]	0.15 ± 0.02 [6.9 ± 0.7]	Sy1.9	0.047	224.5	1.28	0	0.24 (0.1–2.4) 23.2 (20–100)
IGR J18244−5622	1.16 ± 0.09 [1.41 ± 0.11]	0.14 ± 0.05 [0.16 ± 0.05]	3.05 ± 0.16 [3.9 ± 0.2]	Sy2	0.017	79.4	0.09	1.17	0.83 (2–10)

* heavily blended with [N II] lines

IGR J14552−5133 (Fig. 2, upper left panel) include other objects, besides the ones we identify here as their optical counterparts. Optical spectroscopy demonstrates that these other objects are normal Galactic stars, therefore unrelated with the high energy emission detected by *INTEGRAL*.

We recall that, as mentioned in Sect. 2, the putative optical counterparts of hard X-ray sources IGR J14175−4641, IGR J14552−5133 and IGR J18244−5622 (Revnivtsev et al. 2006a,b) were not chosen via soft X-ray catalogues cross-correlation. We also remark that the first and the third of these cases completely lack a catalogued arcsec-sized X-ray counterpart position, while the second one contains three *ROSAT* sources within the IBIS error circle (with that associated with the selected putative optical counterpart being the closest to the centre of the IBIS error box). Therefore, the counterparts we propose for them, although likely, need confirmation through pointed soft X-ray observations with satellites affording arcsecond localizations (such as *Chandra*, *XMM-Newton* or *Swift*). Keeping in mind all of the above, from now on we will nevertheless consider as true the optical/hard X-ray association regarding these three sources.

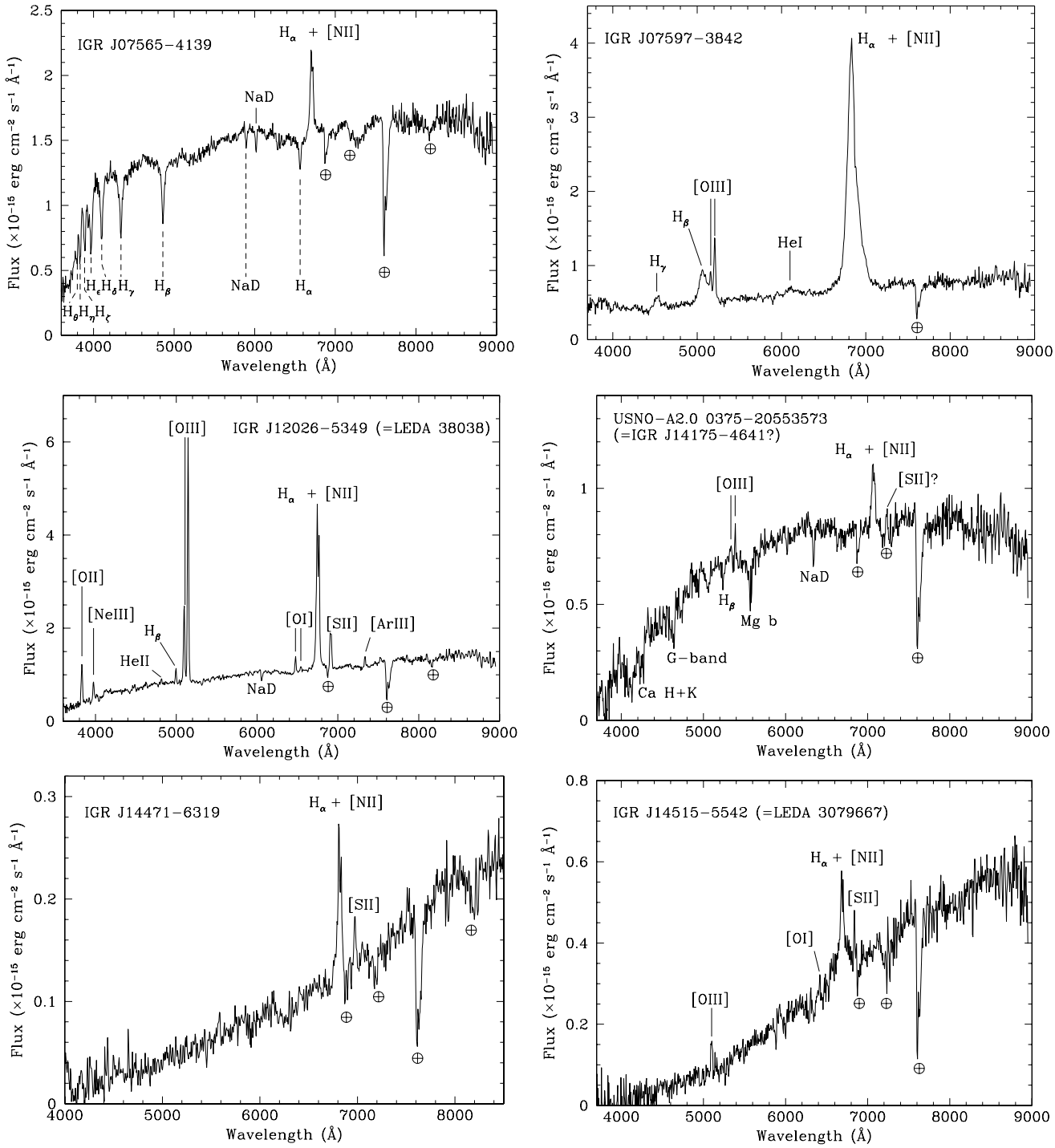

Fig. 5. Spectra (not corrected for the intervening Galactic absorption) of the optical counterparts of 6 AGNs identified in this sample; all spectra were acquired with the 1.5 m CTIO telescope. For each spectrum the main spectral features are labeled. The symbol ⊕ indicates atmospheric telluric absorption bands. We remark that USNO-A2.0 object 0375−20553573 should be considered as the tentative, although likely, counterpart of IGR J14175−4641 (see text). The dashed lines in the spectrum of IGR J07565−4139 indicate absorption features at $z = 0$, likely produced by an interloping Galactic star.

Going into details concerning some objects, for two Seyfert 2 AGNs the available soft X-ray information (Sazonov et al. 2005; Revnivtsev et al. 2006b), together with the local absorption estimate obtained from the optical spectra (see Table 5), allows us to determine their Compton regime (see Bassani et al. 1999, for details). Using the [OIII] λ5007 line fluxes corrected for the total (Galactic plus local to the AGN) absorption, we find that IGR J12026−5349 has a [OIII]/(2−10 keV) flux ratio of 0.8, indicating that it is a Compton thick source, whereas this same parameter is 5.0 for IGR J18244−5622, telling us that this is a Seyfert 2 AGN in the Compton thin regime. In this respect, we remark that observations with satellites sensitive to the 2−10 keV emission are needed for the other sources in Table 5 lacking information in this X-ray band in order to definitely determine their Compton nature. For some of them, an analysis of the *Swift* data is now underway (Landi et al., in preparation).

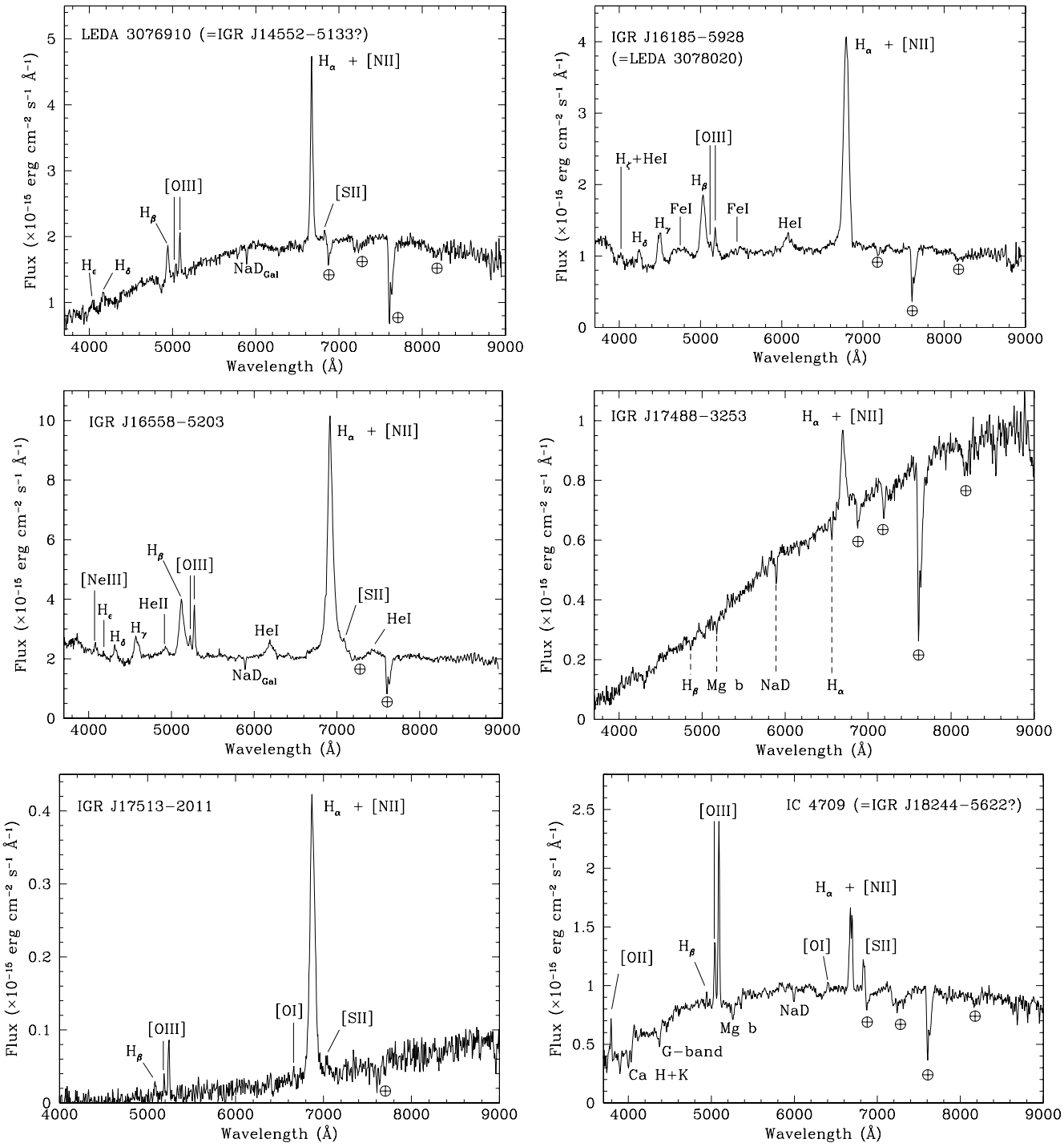

Fig. 6. As Fig. 5, but for the remaining 6 AGNs identified in this sample. We remark that galaxies LEDA 3076910 and IC 4709 should be considered as tentative, although likely, counterparts of IGR J14552−5133 and IGR J18244−5622, respectively (see text). The dashed lines in the spectrum of IGR J17488−3253 indicate absorption features at $z = 0$, likely produced by an interloping Galactic star.

It is also noticeable that the spectra of IGR J07565−4139 and, to a lesser extent, IGR J17488−3253 appear as "hybrid", i.e. with features of both a Galactic star and of an AGN (the former ones are indicated with dashed lines in Fig. 5, upper left panel and in Fig. 6, central right panel). In this sense, they are evidently similar to the case of IGR J20247+5058 (Paper I), and can be interpreted as the chance superposition of a nearby star and a background AGN. High-resolution imaging is thus desirable to disentangle the Galactic star contribution for these two objects.

Moreover, as already mentioned, we tentatively classify IGR J14552−5133 and IGR J16185−5928 as NL Seyfert 1 AGNs following the criteria of Osterbrock & Pogge (1985), although the Fe II bumps are not readily detected in IGR J14552−5133 and the Full Width at Half Maximum (FWHM) of H_β emission in IGR J16185−5928 is ∼4000 km s^{-1}, i.e. twice as the maximum expected for a NL Seyfert 1 AGN.

To conclude this section, following Wu et al. (2004) and Kaspi et al. (2000), we can compute an estimate of

the mass of the central black hole in 5 of the 6 objects classified as Seyfert 1 AGN (this procedure could not be applied to IGR J17488−3253 as no H_β emission was detected). The broad-line region (BLR) gas velocities v_{BLR} (measured from the H_β emission line FWHM) and the corresponding black hole masses for these 5 cases are reported in Table 6.

4.4. Statistical considerations

We can now briefly recover the statistical approach made in Paper II, updating the numbers presented there with recent discoveries (Papers III and IV; Masetti et al. 2006e,f; Halpern & Gotthelf 2006; Negueruela & Smith 2006) and with the sample of sources illustrated in the present work. It is now found that, presently, of the 54 *INTEGRAL* sources identified through optical spectroscopy, 22 (41%) are X-ray binaries (with a large majority, i.e. more than 90%, of HMXB), 24 (44%) are AGNs (half of which were presented in this paper for the first time) and 8 (15%) are CVs (5 of which were shown here for the first time), with at least 6 of them belonging to the IP subclass (see Paper IV and the present work).

One can compare, for instance, these numbers with those for the group of the 153 identified objects belonging to the largest catalogue of *INTEGRAL* sources published up to now, i.e., the 2nd IBIS Galactic Plane Survey (Bird et al. 2006). In this survey we have 107 (70%) X-ray binaries (of which, only one third are HMXBs), 27 (18%) AGNs and 8 (5%) CVs, with at least 6 of them of magnetic nature (IPs or Polars).

From these numbers, graphically reported in percentage terms in the histogram in Fig. 7, one can immediately see that the CV sample detected with *INTEGRAL* has been doubled thanks to the optical spectroscopy identification approach. This also stresses *INTEGRAL*'s sensitivity in detecting hard X-ray emission from this class of objects. One of the reasons for this may be found in the fact that the bulk of the X-ray emission from magnetic CVs falls in the 20−40 keV band (e.g., de Martino et al. 2004; Suleimanov et al. 2005), which is the one in which *INTEGRAL* has the strongest sensitivity. A thorough description of CVs detected by *INTEGRAL* up to now can be found in Barlow et al. (2006).

The number of *INTEGRAL*-detected AGNs also has nearly doubled thanks to these optical studies; besides, it is apparent that an important fraction of the *INTEGRAL* sources identified by means of optical spectroscopy and lying on the Galactic Plane is composed of background AGNs. This once again underscores the extraordinary capabilities of *INTEGRAL* of piercing through the Zone of Avoidance of the Galaxy for the exploration of this part of the extragalactic sky.

As a final corollary, we would like here to stress the extreme effectiveness of the strategy of catalogues cross-correlation plus optical spectroscopy we are pursuing to securely pinpoint the actual nature of the X-ray sources detected with *INTEGRAL*: for instance, of the 56 unidentified objects belonging to the 2nd IBIS Galactic Plane Survey (Bird et al. 2006), this observational approach led to the discovery of the nature of 18 sources (10 AGNs, 6 HMXBs and 2 CVs), i.e., nearly one third of the total, 15 of which being reported in our Papers II−IV and in the present work. The corresponding source type percentages are represented as shaded areas in Fig. 7.

The lack of known accurate (up to ∼10 arcsec) soft X-ray position is the main cause of failure in this identification task; therefore, observations with high-resolution imaging X-ray satellites (such as *Chandra*, *XMM-Newton* and/or *Swift*) are of paramount importance for the continuation of this program aimed at identifying the nature of unknown *INTEGRAL* hard X-ray sources.

Table 6. BLR gas velocities (in km s^{-1}) and central black hole masses (in units of 10^7 $M_\odot$) for 5 Seyfert 1 AGNs belonging to the sample presented in this paper.

Object	v_{BLR}	M_{BH}
IGR J07597−3842	5500	20
IGR J14552−5133	1600	0.2
IGR J16185−5928	3500	2.8
IGR J16558−5203	2900	7.8
IGR J17513−2011	1100	0.1

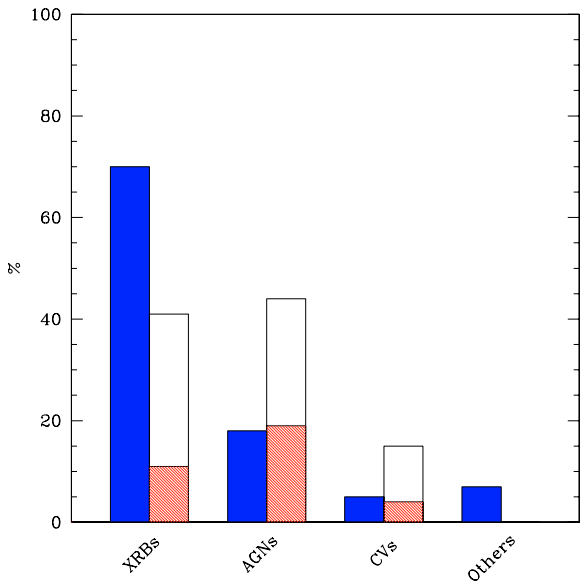

Fig. 7. Histogram, subdivided into source types, showing the percentage of *INTEGRAL* objects of known nature and belonging to the 2nd IBIS Galactic Plane Survey (Bird et al. 2006; left-side, darker columns), and *INTEGRAL* sources from various surveys and identified through optical spectroscopy (right-side, lighter columns). The latter columns also show (as shaded areas) the percentage of sources identified thanks to optical spectroscopy and which belong to 2nd IBIS Galactic Plane Survey.

5. Conclusions

In our continuing work of identification of *INTEGRAL* sources by means of optical spectroscopy (Papers I−IV), we have identified and studied 21 southern hard X-ray objects of unknown nature by means of the 1.5 m CTIO telescope of Cerro Tololo (Chile).

We found that the selected sample is made of 12 AGNs (6 of which are of Seyfert 1 type and 6 are Seyfert 2 AGNs), 5 magnetic CVs and 4 HMXBs (one of which in the LMC). In terms of relative sizes of the three groups, we notice the absolute majority of AGNs in the sample, and a comparatively large fraction (∼25%) of CVs.

We recall that in three cases (IGR J14175−4641, IGR J14452−5133 and IGR J18244−5622), all identified as AGNs, only a tentative albeit likely optical counterpart was given because of the the lack of an univocal arcsecond-sized soft X-ray position. Thus, for them an observation with soft X-ray satellites affording arcsecond localizations (such as *Chandra*, *XMM-Newton* or *Swift*) is needed to confirm the proposed association.

The results presented in this work further indicate the capabilities of *INTEGRAL* to reveal not only high- and low-mass X-ray binaries, but also (if not mostly) extragalactic objects in the nearby Universe ($z < 0.1$) and magnetic dwarf novae.

Acknowledgements. We thank Claudio Aguilera and Arturo Gómez for the daily and nightly assistance at the telescope, and the anonymous referee for useful remarks which helped us to improve the paper. This research has made use of the NASA Astrophysics Data System Abstract Service, of the NASA/IPAC Extragalactic Database (NED), and of the NASA/IPAC Infrared Science Archive, which are operated by the Jet Propulsion Laboratory, California Institute of Technology, under contract with the National Aeronautics and Space Administration. This publication makes use of data products from the Two Micron All Sky Survey (2MASS), which is a joint project of the University of Massachusetts and the Infrared Processing and Analysis Center/California Institute of Technology, funded by the National Aeronautics and Space Administration and the National Science Foundation. This research has also made use of the SIMBAD database operated at CDS, Strasbourg, France, and of the HyperLeda catalogue operated at the Observatoire de Lyon, France. The authors acknowledge the ASI and INAF financial support via grant No. 1/023/05/0. N.M. thanks the Departamento de Astronomía y Astrofísica of the Pontificia Universidad Católica de Chile for the pleasant hospitality during the preparation of this paper. L.M.'s work is supported by the Fondap Center for Astrophysics grant No. 15010003.

References

Barlow, E. J., Knigge, C., Bird, A. J., et al. 2006, MNRAS, in press [arXiv:astro-ph/0607473]
Bassani, L., Dadina, M., Maiolino, R., et al. 1999, ApJS, 121, 473
Bird, A. J., Barlow, E. J., Bassani, L., et al. 2006, ApJ, 636, 765
Bikmaev, I. F., Revnivtsev, M. G., Burenin, R. A., & Sunyaev, R. A. 2006, Astron. Lett., 32, 588
Cardelli, J. A., Clayton, G. C., & Mathis, J. S. 1989, ApJ, 345, 245
Cusumano, G., Israel, G. L., Mannucci, F., et al. 1998, A&A, 337, 772
den Hartog, P. R., Hermsen, W., Kuiper, L., et al. 2006, A&A, 451, 587
de Martino, D., Matt, G., Belloni, T., Haberl, F., & Mukai, K. 2004, A&A, 415, 1009
Dean, A. J., Bazzano, A., Hill, A. B., et al. 2005, A&A, 443, 485
Götz, D., Mereghetti, S., Merlini, D., Sidoli, L., & Belloni, T. 2006, A&A, 448, 873
Gros, A., Goldwurm, A., Cadolle-Bel, M., et al. 2003, A&A, 411, L179
Halpern, J. P. 2005, ATel 572
Halpern, J. P., & Gotthelf, E. V. 2006, ATel 692
Halpern, J. P., & Mirabal, N. 2006, ATel 709
Hamuy, M., Walker, A. R., Suntzeff, N. B., et al. 1992, PASP, 104, 533
Hamuy, M., Suntzeff, N. B., Heathcote, S. R., et al. 1994, PASP, 106, 566
Ho, L. C., Filippenko, A. V., & Sargent, W. L. W. 1993, ApJ, 417, 63
Ho, L. C., Filippenko, A. V., & Sargent, W. L. W. 1997, ApJS, 112, 315
Horne, K. 1986, PASP, 98, 609
Kaspi, S., Smith, P. S., Netzer, H., et al. 2000, ApJ, 533, 631
Kuiper, L., Keek, S., Hermsen, W., Jonker, P. G., & Steeghs, D. 2006, ATel 684
Lang, K. R. 1992, Astrophysical Data: Planets and Stars (New York: Springer-Verlag)
Leitherer, C. 1988, ApJ, 326, 356
Masetti, N., Palazzi, E., Bassani, L., Malizia, A., & Stephen, J. B. 2004, A&A, 426, L41 (Paper I)
Masetti, N., Mason, E., Bassani, L., et al. 2006a, A&A, 448, 547 (Paper II)
Masetti, N., Pretorius, M. L., Palazzi, E., et al. 2006b, A&A, 449, 1139 (Paper III)
Masetti, N., Bassani, L., Bazzano, A., et al. 2006c, A&A, 455, 11 (Paper IV)
Masetti, N., Morelli, L., Palazzi, E., et al. 2006d, ATel 783
Masetti, N., Bassani, L., Dean, A. J., Ubertini, P., & Walter, R. 2006e, ATel 715
Masetti, N., Bassani, L., Bazzano, A., et al. 2006f, ATel 815
Massey, P. 2002, ApJS, 141, 81
Negueruela, I., & Smith, D. M. 2006, ATel 831
Osterbrock, D. E. 1989, Astrophysics of Gaseous Nebulae and Active Galactic Nuclei (Mill Valley: Univ. Science Books)
Osterbrock, D. E., & Pogge, R. W. 1985, ApJ, 297, 166
Revnivtsev, M., Sazonov, S. Y., Molkov, S. V., et al. 2006a, Astron. Lett., 32, 145
Revnivtsev, M., Sazonov, S. Y., Churazov, E. M., & Trudolyubov, S. 2006b, A&A, 448, L49
ROSAT Team 2000, *ROSAT* News No. 71, The *ROSAT* Source Catalog of Pointed Observations with the High Resolution Imager (1RXH; 3rd Release)
Sazonov, S. Y., Churazov, E., Revnivtsev, M. G., Vikhlinin, A., & Sunyaev, R. A. 2005, A&A, 444, L37
Schlegel, D. J., Finkbeiner, D. P., & Davis, M. 1998, ApJ, 500, 525
Skrutskie, M. F., Cutri, R. M., Stiening, R., et al. 2006, AJ, 131, 1163
Stephen, J. B., Bassani, L., Molina, M., et al. 2005, A&A, 432, L49
Stephen, J. B., Bassani, L., Malizia, A., et al. 2006, A&A, 445, 869
Suleimanov, V., Revnivtsev, M., & Ritter, H. 2005, A&A, 435, 191
Tomsick, J. A., Chaty, S., Rodriguez, J., et al. 2006, ApJ, 647, 1309
Ubertini, P., Lebrun, F., Di Cocco, G., et al. 2003, A&A, 411, L131
Veilleux, S., & Osterbrock, D. E. 1987, ApJS, 63, 295
Voges, W., Aschenbach, B., Boller, T., et al. 1999, A&A, 349, 389
Voges, W., Aschenbach, B., Boller, T., et al. 2000, IAU Circ., 7432
Walter, R., Zurita Heras, J., Bassani, L., et al. 2006, A&A, 453, 133
Warner, B. 1995, Cataclysmic variable stars (Cambridge: Cambridge Univ. Press)
Wegner, W. 1994, MNRAS, 270, 229
Winkler, H. 1992, MNRAS, 257, 677
Winkler, C., Courvoisier, T. J.-L., Di Cocco, G., et al. 2003, A&A, 411, L1
Wu, X.-B., Wang, R., Kong, M. Z., Liu, F. K., & Han, J. L. 2004, A&A, 424, 793

Online Material

Table 1. Log of the spectroscopic observations presented in this paper.

Object	Date	Mid-exposure time (UT)	Exposure time (s)
IGR J05007−7047	21 Mar. 2006	00:35:17	2×1200
IGR J07565−4139	21 Mar. 2006	01:42:08	2×1200
IGR J07597−3842	21 Mar. 2006	02:39:12	2×1200
IGR J10101−5654	06 Apr. 2006	03:05:43	2×1800
IGR J12026−5349	21 Mar. 2006	03:46:53	2×1800
XSS J12270−4859	22 Mar. 2006	01:32:07	2×1800
IGR J14175−4641	21 Mar. 2006	04:44:08	2×1200
IGR J14471−6319	06 Apr. 2006	04:23:39	2×1800
IGR J14515−5542	22 Mar. 2006	03:21:20	2×1800
IGR J14536−5522	22 Mar. 2006	04:21:53	2×1200
IGR J14552−5133	22 Mar. 2006	05:40:02	1800
IGR J15094−6649	22 Mar. 2006	06:50:21	1800 + 1200
IGR J16167−4957	21 Mar. 2006	06:03:46	2×1800
IGR J16185−5928	22 Mar. 2006	08:02:00	2×1800
IGR J16207−5129	23 Mar. 2006	06:33:05	2×1800
IGR J16558−5203	21 Mar. 2006	07:26:17	2×1200
IGR J17195−4100	21 Mar. 2006	08:39:00	2×1800
IGR J17200−3116	06 Apr. 2006	05:34:33	2×1500
IGR J17488−3253	04 Apr. 2006	07:11:21	2×2400
IGR J17513−2011	04 Apr. 2006	08:53:27	2×2700
IGR J18244−5622	05 Apr. 2006	09:35:21	2×1200

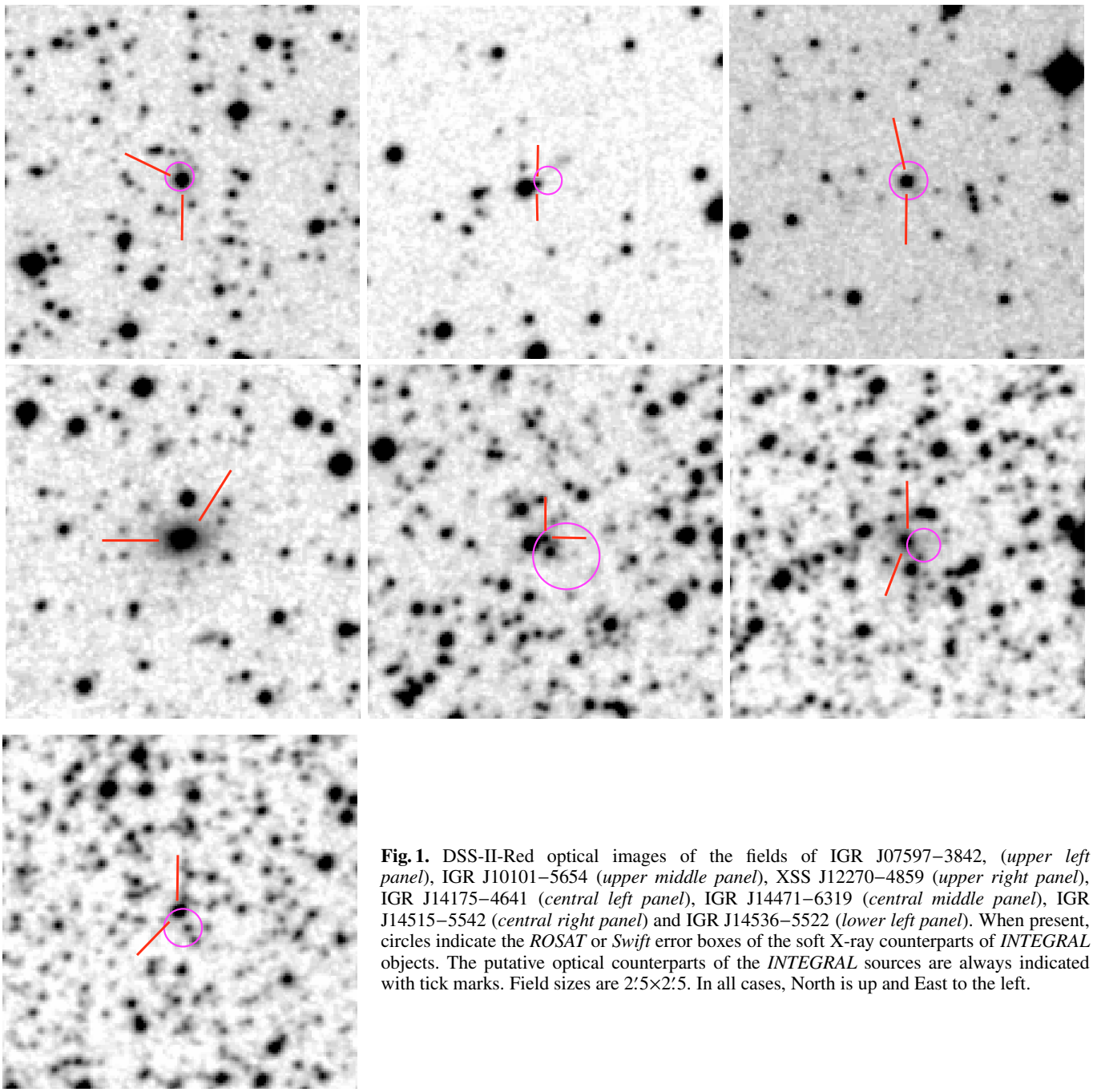

Fig. 1. DSS-II-Red optical images of the fields of IGR J07597−3842, (*upper left panel*), IGR J10101−5654 (*upper middle panel*), XSS J12270−4859 (*upper right panel*), IGR J14175−4641 (*central left panel*), IGR J14471−6319 (*central middle panel*), IGR J14515−5542 (*central right panel*) and IGR J14536−5522 (*lower left panel*). When present, circles indicate the *ROSAT* or *Swift* error boxes of the soft X-ray counterparts of *INTEGRAL* objects. The putative optical counterparts of the *INTEGRAL* sources are always indicated with tick marks. Field sizes are 2′.5×2′.5. In all cases, North is up and East to the left.

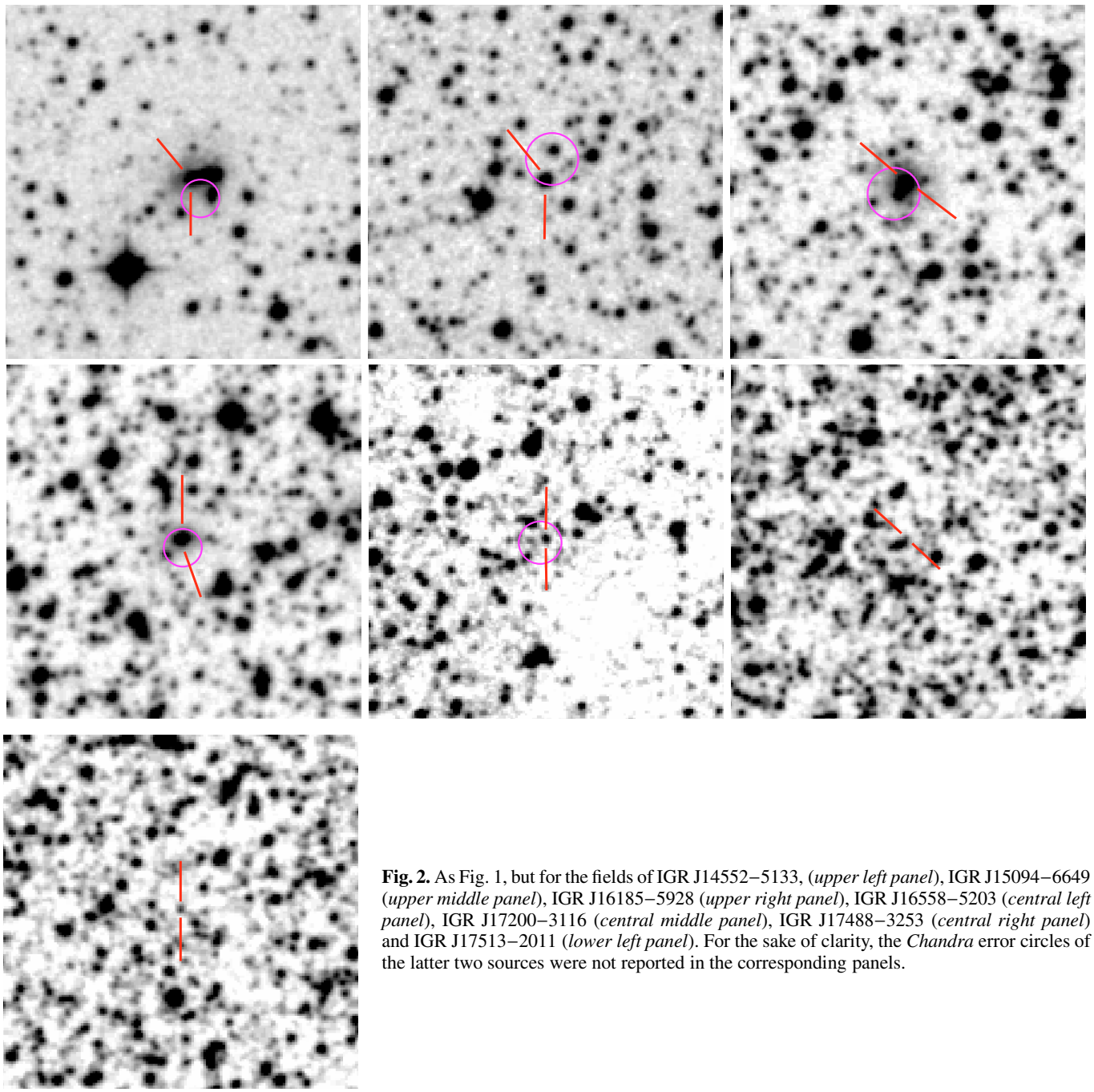

Fig. 2. As Fig. 1, but for the fields of IGR J14552−5133, (*upper left panel*), IGR J15094−6649 (*upper middle panel*), IGR J16185−5928 (*upper right panel*), IGR J16558−5203 (*central left panel*), IGR J17200−3116 (*central middle panel*), IGR J17488−3253 (*central right panel*) and IGR J17513−2011 (*lower left panel*). For the sake of clarity, the *Chandra* error circles of the latter two sources were not reported in the corresponding panels.